RESEARCH PAPER

Magnetic Graphene Quantum Dots as a Functional Nanomaterial Towards Voltammetric Detection of L-tryptophan at Physiological pH

Mohammad Hasanzadeh [1] , Ayub Karimzadeh [2] and Nasrin Shadjou [3,4]*

[1] *Drug Applied Research Center, Tabriz University of Medical Sciences, Tabriz 51664, Iran*
[2] *Pharmaceutical Analysis Research Center, Tabriz University of Medical Sciences, Tabriz 51664, Iran*
[3] *Department of Nanochemistry, Nano Technology Research Center, Urmia University, Urmia 57154, Iran*
[4] *Department of Nano Technology, Faculty of Science, Urmia University, Urmia 57154, Iran*

ARTICLE INFO

Article History:
Received 28 October 2017
Accepted 12 December 2017
Published 01 January 2018

Keywords:
Amino acid
Graphene quantum dot
L-Tryptophan
Magnetic nanoparticle

ABSTRACT

L-Tryptophan (L-Trp) is of great importance in the biochemical, pharmaceutical and dietetic fields as it is precursor molecule of some hormones, neurotransmitters and other relevant biomolecules. So, determination of this amino acid has important role in detection of some neuron based disease. The main purpose of this report was to develop application of Fe_3O_4 magnetic nanoparticles/graphene quantum dots (Fe_3O_4 MNP-GQDs)) as a nanosensor towards electrooxidation and determination of L-Trp and also the evaluation its kinetic parameters. In continuation of our efforts to use Fe_3O_4 MNP-GQDs for amino acids detection, our objective in the present work was to expand application of this sensor for the determination of L-Trp which is very sensitive. Decrease in oxidation overpotential and enhancement in current proved the electrocatalytic activity of Fe_3O_4 MNPs-GQDs-GCE as a sensor. Importantly, by this simple method of fabrication a much lower detection limit was achieved without involving any pre-treatment or activation steps. The analytical applicability of the modified electrode has been evaluated by successfully employing it for the determination of L-Trp in the standard solution.

How to cite this article
Hasanzadeh M, Karimzadeh A, Shadjou N. Magnetic Graphene Quantum Dots as a Functional Nanomaterial Towards Voltammetric Detection of L-tryptophan at Physiological pH. J Nanostruct, 2018; 8(1): 21-30. DOI: 10.22052/JNS.2018.01.003

INTRODUCTION

Tryptophan (Trp) is an essential amino acid for humans and herbivores scarcely present in vegetable products. It is a vital constituent of proteins and indispensable to human nutrition for establishing and maintaining a positive nitrogen balance. Tryptophan is also a precursor of the neurotransmitter serotonin [1]. Therefore, Trp is of great importance in the biochemical, pharmaceutical and dietetic fields as it is precursor molecule of some hormones, neurotransmitters and other relevant biomolecules [2]. It has been implicated as a possible cause of schizophrenia in people who cannot metabolize it properly. When improperly metabolized, it creates a waste product in the brain that is toxic, causing hallucinations and delusions [3]. So, determination of this amino acid has important role in detection of some neuron based disease.

Several methods that have been used for the determination of Trp in different samples include chromatography, chemiluminescence, spectrophotometry, fluorimetry, flow injection analysis and electrophoresis [4, 5]. Nevertheless,

* *Corresponding Author Email: hasanzadehm@tbzmed.ac.ir*

these methods are complex, time-consuming, expensive and often suffer from selectivity or specificity and pretreatment or require derivatization prior to its determination. [6] Trp being an electroactive compound, electroanalytical techniques provide an alternate way to analyze Trp with certain advantages such as quick response, high sensitivity, high selectivity, and inexpensiveness, amenability to miniaturization, low power consumption and wide linear dynamic range [7]. However, the electrochemical detection of Trp faces some problems. At traditional working electrodes, Trp follows a sluggish kinetics and has very high oxidation overpotential. [8, 9] The other electroactive biomolecules which coexist with Trp in biological matrices interfere with the determination of Trp due to their similar oxidation peak potentials. These problems are solved by modifying the electrodes with suitable materials using various modification methods. [10] Many materials have been used to modify the traditional working electrodes for the determination of Trp [11].

Recently, we developed a one-step electrodeposition method for the electrosynthesis of Fe_3O_4 MNP-GQDs on the surface of GCE [12]. Using this simple and effective deposition method, GQDs can be effectively coated on the surface of electrode. The as-prepared Fe_3O_4 MNP-GQDs shows favorable electroactivity towards some amino acids (L-Cysteine, L-Tyrosine, L-Aspartic acid, and L-Phenylalanine) oxidation.

Based on outstanding electroactivity of Fe_3O_4 MNP-GQDs modified GCE towards determination of some amino acids and at continuing our previously report[12], in this communication the performance of Fe_3O_4 MNP-GQDs-GCE was evaluated towards electrooxidation and determination of L-Trp. The aim of this communication is merely to expand application of Fe_3O_4 MNP-GQDs-GCE towards the kinetic and analytical investigates L-Trp.

MATERIALS AND METHODS

Chemicals and reagents

All chemicals were purchased from Merck (Darmstadt, Germany) and used without further purification. Alumina slurry was purchased from Beuhler (Illinois, USA) and raw material of L-Trp was purchased from Merck (Germany). All solutions were prepared with deionized water. The stock solution of L-Trp (0.003 g/ mL) was prepared by dissolving an accurate amount of L-Trp in an appropriate volume of 0.1 M phosphate buffer solution (PBS), pH=7.4 (which was also used as supporting electrolyte), and then stored in the dark place at 4°C. Additional dilute solutions were prepared daily by accurate dilution just before use. Also the other stock solutions were prepared by dissolving an accurate amount equal to molecular weight of each one in an appropriate volume of 1000 mL deionized water and then all stored in the dark place at 4 °C.

Apparatuses and methods

Electrochemical measurements were carried out in a three-electrode cell setup. The system was run on a Personal Computer using NOVA1.7 software. Saturated Ag/AgCl as a reference electrode and the counter electrode (also known as auxiliary electrode), which usually made of an inert material was platinum. All potentials were measured with respect to the Ag/AgCl which was positioned as close to the working electrode as possible by means of a luggin capillary. Glassy carbon electrode (GCE) (from Azar electrode Co., Urmia, Iran) was used as the working electrode. The transmission electron microscope (TEM) images were obtained on Leo 906, Zeiss, (Germany). Atomic force microscopy (AFM) experiments were performed at contact mode by Nanowizard AFM (JPK Instruments AG, Berlin, Germany) mounted on Olympus Invert Microscope IX81 (Olympus Co., Tokyo, Japan).

Synthesis GQDs and Fe_3O_4 MNPs-GQDs

An easy bottom-up method was used for the preparation of GQDs. At first, GQDs were synthesized by pyrolyzing citric acid and dispersing the carbonized products into alkaline solutions. Briefly, 2 g of citric acid was put into a beaker and heated to 200 °C by a heating mantle until the citric acid changed to an orange liquid. Then, for preparing GQDs, 100 mL of 10 mg/mL NaOH solution was added into the orange homogenous liquid dropwise with continuous stirring. The obtained GQD solution was stable for at least one month at 4 °C. Then, The Fe_3O_4 MNPs-GQDs composites were synthesized through a one-step co-precipitation procedure. First, GQDs (0.1 g) was dispersed in 150 mL deionized water by sonication for 10 min. Then, 1.214 g $FeCl_3.6H_2O$ was added to GQDs solution at room temperature under a nitrogen flow with vigorous stirring. Then, temperature was increased to 80 ℃, and 0.485 g

of the $FeCl_2.4H_2O$ was added slowly to the solution containing Fe^{3+}/GQDs, which was vigorously stirred for an additional 30 min. Finally, the ammonia solution was added dropwise to adjust the pH of the solution to 10 for the synthesis of magnetite Fe_3O_4 MNPs-GQDs.

Characterization of GQDs and Fe_3O_4 MNPs-GQDs

Fig. 1(A and B) presents the AFM and TEM images of synthesized GQDs. The corresponding AFM image shows a single GQD monolayer thin film. Ninety percent of the particles represent dark brown color which assigned to a size range below 10 nm. Also, the morphologies of the Fe_3O_4 MNPs-GQDs used in this work were characterized using AFM and TEM and the images are depicted in Fig. 1D and E. From these images it's found that, differing from the two dimensional layered structures of GQDs, the Fe_3O_4 MMNPs and GQDs aggregated into three dimensional structures. Most probably, as schematically depicted in Fig. 1D-F, the Fe_3O_4 MNPs are surrounded by GQDs to form composite particles. The sizes of the Fe_3O_4 MNPs-GQDs particles reached 30 nm.

In addition, the surface chemistry of Fe_3O_4 MNPs-GQDs was investigated using FTIR. The typical FT-IR spectra of magnetic nanoparticles are shown in Fig. 2. As can be seen the Fe–O band at Fe_3O_4 MNPs-GQDs (611 cm^{-1}) shifted to a higher wavelength in comparison with Fe_3O_4 (580 cm^{-1}), indicating the bonding of Fe_3O_4 to C–O–H groups on the GQDs surface. An absorption bond appeared at 3411 cm^{-1} corresponding to hydroxyl groups on Fe_3O_4 and the Fe_3O_4 MNPs-GQDs surface and a peak at 1618 cm^{-1} corresponded to the vibration of water molecules adsorbed on Fe_3O_4 and Fe_3O_4 MNPs-GQDs surfaces. A strong bond at 1605 cm^{-1} corresponded to the stretching frequencies of C-C on the Fe_3O_4 MNPs-GQDs surface. Peaks at 908 cm^{-1} and 1065 cm^{-1} can be attributed to the stretching frequencies of C–C on Fe_3O_4 MNPs-GQDs and the peaks at 1258 cm^{-1} and 1384 cm^{-1} corresponded to the C–O stretching and O–H bending vibrations.

Preparation of GQDs and Fe_3O_4 MNPs-GQDs modified GCE (GQDs-GCE and Fe_3O_4 MNPs-GQDs-GCE)

GCE (2 mm in diameter) was polished to a mirror-like finish with 0.3 and 0.05 µm alumina slurry and then thoroughly rinsed with double distilled water. Then it was successively sonicated

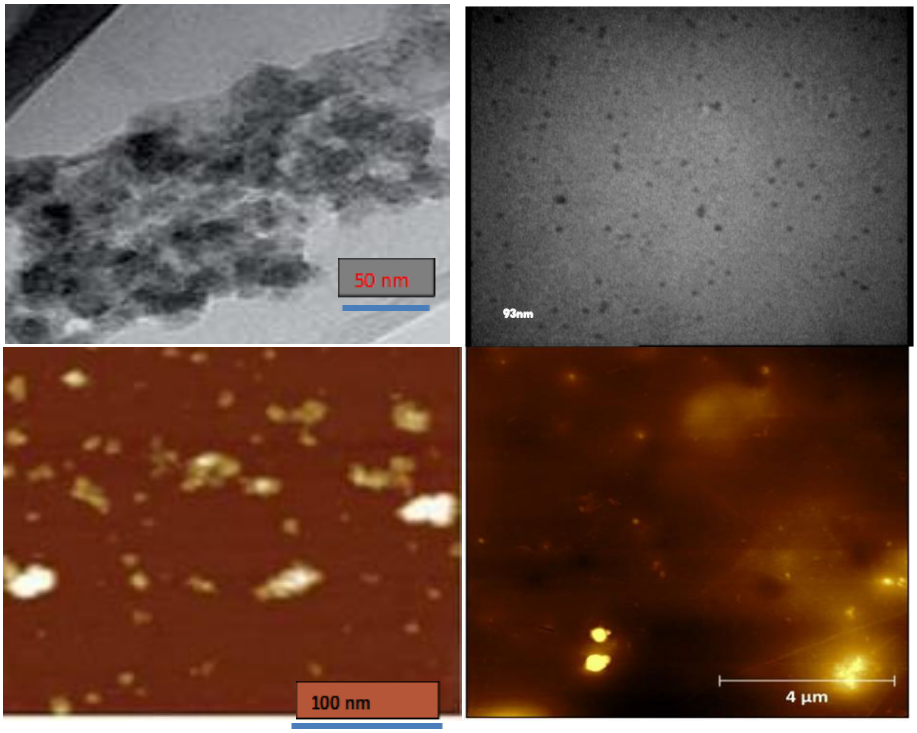

Fig. 1. TEM, and AFM images of the GQDs and Fe_3O_4 MNPs-GQDs.

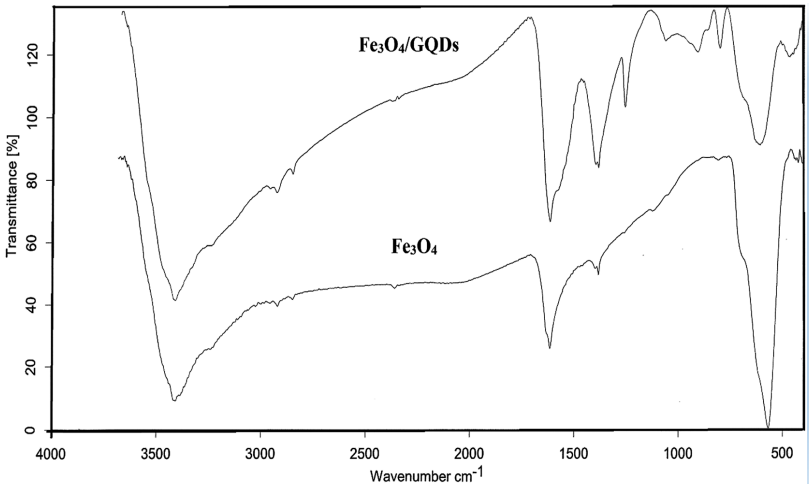

Fig. 2. FT-IR spectra of Fe_3O_4 MNPs and Fe_3O_4 MNPs-GQDs.

in acetone and double distilled water and was allowed to dry at room temperature. Finally, 5 mL homogenous GQD and Mag-GQD films were electrodeposited onto GCE by cyclic voltammetry (CV) in the potential range from -1.0 to 1.0 V at a scan rate of 200 mV s^{-1} for 30 cycles (Fig. 3). When the cyclic potential scan reached 30 cycles, the peak currents hardly changed. The first positive scan, an oxidation peak (I) at + 0.51 V was observed, which is attributed to the oxidation of the Fe_3O_4 MNPs-GQDs. In the subsequent reversal scan, one reduction peaks (II) were observed at -0.7 V, which may be attributed to the reduction of species. In addition, it's found that, peak I was decreased cycle by cycle, and reflecting the continuous growth of the Fe_3O_4 MNPs-GQDs on the surface of GCE. These facts indicate that Fe_3O_4 MNPs-GQDs was successfully deposited on the surface of GCE by the electrochemical method.

After electrochemical deposition of Fe_3O_4 MNPs-GQDs on the GCE, the Fe_3O_4 MNPs-GQDs -GCE was employed for taking SEM images for monitoring the distribution of Fe_3O_4 MNPs and morphology of the engineered electrode surface. The SEM images of the engineered electrode surface have been shown in Fig. 4 at different magnitudes. This Figure shows that magnetic nanoparticles were distributed into GQDs and confirmed attachment of Fe_3O_4 MNPs to the GQDs. Meanwhile the figure shows that some of Fe_3O_4 MNPs have been aggregated. The overall size of Fe_3O_4 MNPs was found to be less than 100 nm. The Fe_3O_4 MNPs were well dispersed on the electrode surface. The effective surface area was 0.098, 0.12 and 0.289 cm^2 for GCE, GQDs-GCE, and Fe_3O_4 MNPs-GQDs-GCE, respectively.

RESULTS AND DISCUSSION

The cyclic voltammograms of GCE, GQDs-GCE and Fe_3O_4 MNP-GQDs-GCE were recorded between -1.0 and 1.0 V using the scan rate of 100 mVs^{-1} in the 0.1 M PBS (pH=7.4) in the presence of L-Trp. As seen in Fig. 5A-C, on the bare GCE electrode (curve a) no redox behavior was observed. On the other hand, as well as on the GQDs-GCE and Fe_3O_4 MNP-GQDs-GCE (curves band c) one pair redox peaks was appeared at 0.14V vs. Ag/AgCl. The comparison of recorded CVs using GQDs-GCE and Fe_3O_4 MNP-GQDs-GCE in the presence of L-Trp (Fig 5C) shows a new anodic peak at 0.657 V on the surface of Fe_3O_4 MNP-GQDs-GCE which attribute to the anodic oxidation of L-Trp using Fe_3O_4 MNP-GQDs-GCE. Therefore, Fe_3O_4 MNP-GQDs-GCE is a suitable mediator to shuttle electron between L-Trp and working electrode, and facilitate electrochemical regeneration following electron exchange with L-Trp.

Typical cyclic voltammograms (CVs) L-Trp on of bare GCE, GQDs-GCE and Fe_3O_4 MNP-GQDs-GCE in 0.1M PBS (pH=7.4) was shown as Fig. 5 where potential sweep rate of 100 mV/s has been employed. According to Fig.1, no oxidation and reduction peaks were observed by using GCE, GQDs-GCE in the absence and presence of L-Trp. On the other hand, the anodic oxidation peak of L-Trp was appeared at about 0.81V. It's important to point out that, in the presence of L-Trp, only one oxidation peak appears at the surface of Fe_3O_4 MNP-

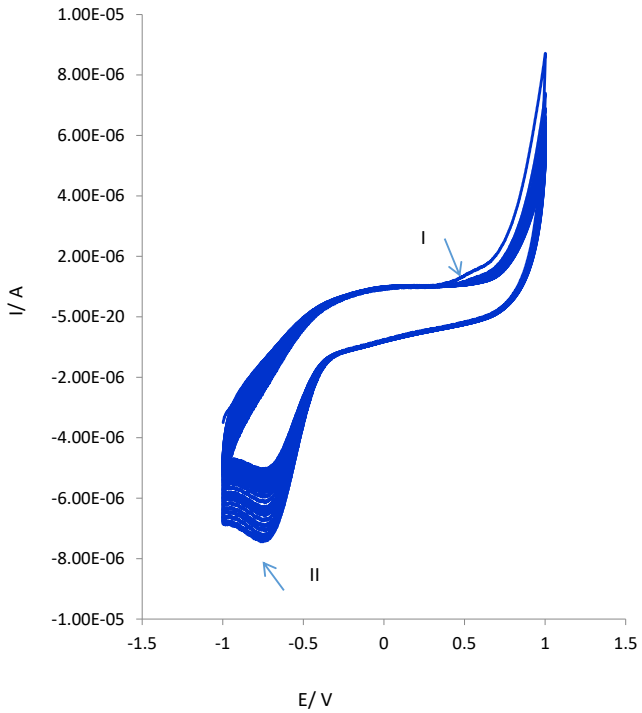

Fig. 3. CVs for 5 mL of Fe3O4 MNP-GQDs using a GC electrode scanned continuously at 200 mVs-1 between -1 to +1 V. Number of scan is 15.

GQDs-GCE. These results indicate that prepared film could accelerate the rate of electron transfer of L-Trp and have good electrocatalytic activity for redox reaction of L-Trp. Also, it showed that no reduction peak was observed in the reverse scan, suggesting that the electrochemical reaction was a totally irreversible process. The data obtained clearly show that the combination of Fe_3O_4 MNP with GQDs definitely improve the characteristics of L-Trp oxidation. That might be related to the excellent property of GQDs, such as high specific surface area and electrical conductivity. The role of Fe_3O_4 MNP was also important for promoting the electrochemical oxidation of L-Trp. Therefore, Fe_3O_4 MNP-GQDs-GCE could be substituted for the oxidation of L-Trp.

Scan rate has an important role in the electrochemical behavior of analytes on the electrode surface. Therefore, the effect of scan rate on the electrochemical response of Fe_3O_4 MNP-GQDs-GCE was investigated at optimum conditions in the presence of L-Trp in PBS (pH=7.4). The scan rate was swept between 2 to 1000 mV/s and the results have been exhibited in Fig. 6A. As it can be seen, the oxidation peak currents increased proportionally by the scan rate indicating that proposed system has suitable potential to shuttling electron. To elucidate the mechanism of mass transfer, two approaches were used. First, the relation between the peak current and square root of scan rate was obtained (Fig. 6B). Using this method, the intercept of the peak current versus the square root of scan rate was found to be 0.00007, which indicates that the mass transfer is controlled by diffusion mechanism rather than adsorption and the system can be applied for quantitative analysis. In the second approach, the Napierian logarithm of peak current versus the Napierian logarithm of scan rate was drawn. The results have been illustrated in Fig. 6C. The slops of the plot in Fig. 2C for oxidation peak were found as 0.3347. If the slop of ln peak current (mA) versus ln scan rate (V/s) is close to 0.5, the process is diffusion controlled; if the slope is close to 1, the process is controlled through adsorptio. As, the slope was calculated as 0.3347, it can be concluded that the mass transfer is a diffusion controlled process which is in agreement with the results of the first approach.

Furthermore, the mass transfer mechanism can also be evaluated by electron transfer coefficient, α, of Eq. 1 [13]:

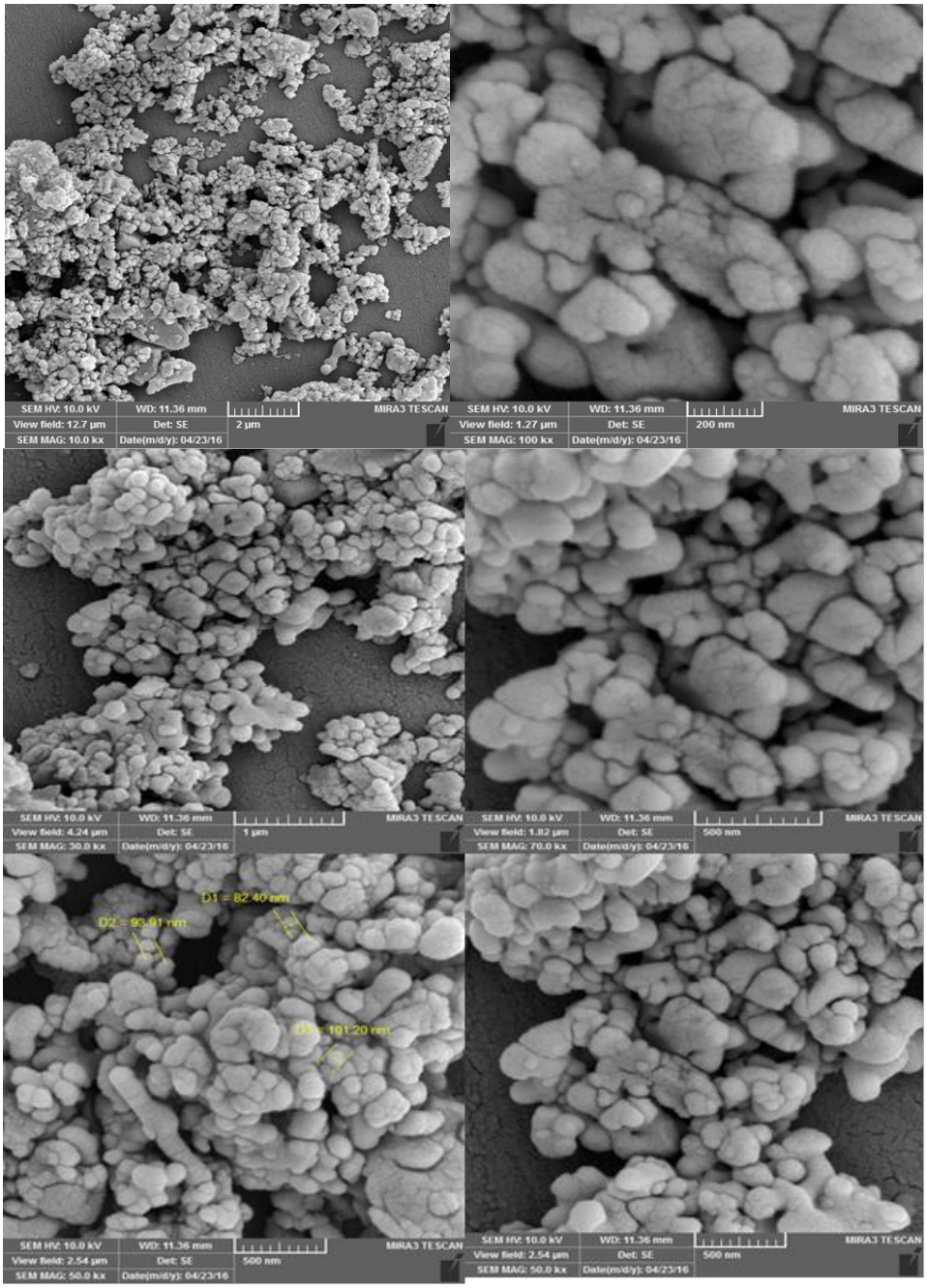

Fig. 4. SEM images of Fe_3O_4 MNP-GQDs modified GC electrode.

$$Ep = \left(\frac{RT}{2\alpha F}\right)\ln \upsilon + constant$$

where E_p is electrode potential, R is gas constant (8.314, J $K^{-1}mol^{-1}$), T is temperature in Kelvin scale (298°K), F is Faraday's constant (96486, A.s.mol^{-1}), and υ is potential sweep rate (V/s). If the value of α gets close to 0.5, the system is a diffusion controlled one. Using this equation, the α value was obtained as 0.33 which further supports that the mass transfer of the system is controlled by diffusion. In Fig. 6D, the plot of Eq. 1 obtained from Napierian logarithm of oxidation peak currents (mA) versus the corresponding peaks potential (V) (Tafel plot) have been illustrated.

In order to develop a voltammetric method

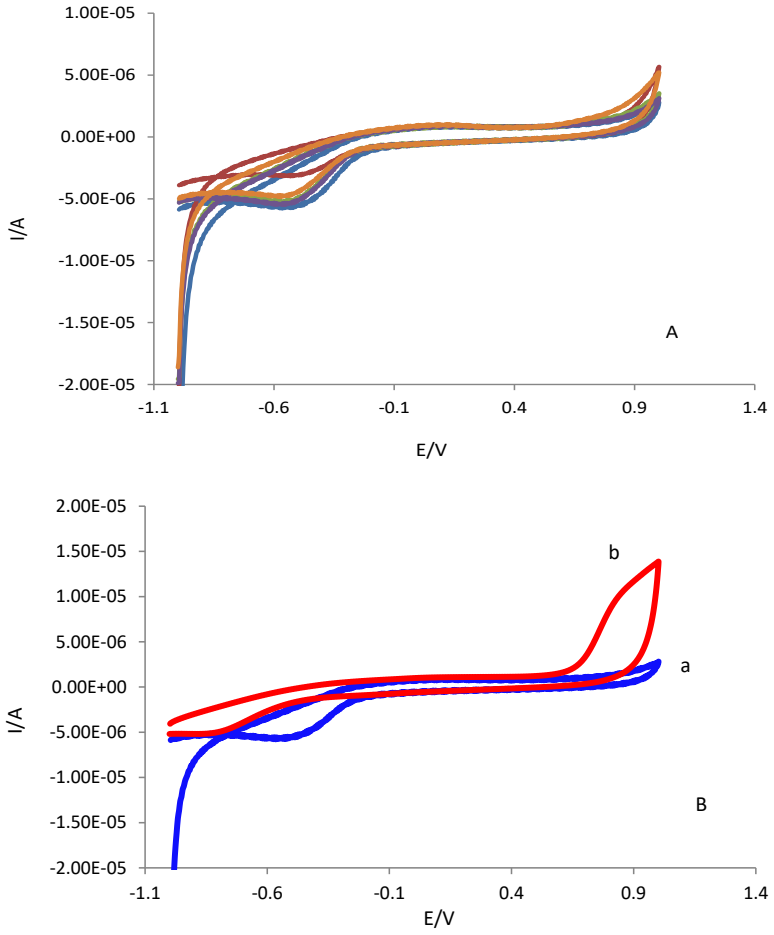

Fig. 5. (A) CVs of GCE, GQDs-GCE and Fe_3O_4 MNP-GQDs-GCE in the absence of L- Trp, (B) CVs of GQDs-GCE (curve a) and Fe_3O_4 MNP-GQDs-GCE (curve b) in the presence of L- Trp (0.004 g/ml)+ 5 ml PBS (0.1M, pH=7.4).

for determining of L-Trp, we selected the DPV mode, because the peaks are sharper and better defined at lower concentration of L-Trp than those obtained by CV, with a lower background current, resulting in improved resolution. According to the obtained results, it was possible to apply this technique to the quantitative analysis of L-Trp. The PBS of pH 7.40 was selected as the supporting electrolyte for the quantification of L-Trp as it gave maximum peak current at pH 7.40. The peak at about 0.7 V was considered for the analysis DPVs obtained with increasing amounts of L-Trp showed that the peak current increased linearly with increasing concentration, as shown in Fig. 7.

Using the optimum conditions described above, linear calibration curves were obtained for L-Trp in the range of 0.5-100 µM. LLOQ was estimated to be 0.1 µM.

It can be seen that the Fe_3O_4 MNPs-GQDs-GCE offered reasonable linear range for L-Trp detection and the detection limit was lower than some of previous reports. These results indicated that Fe_3O_4 MNPs-GQDs-GCE is an appropriate platform for the determination of L-Trp. On the other word, the prepared electrode shows voltammetric responses with low detection limit and wide linear range for L-Trp in optimal conditions, which makes it suitable for determination of this amino acid. It is found that, by incorporating Fe_3O_4 MNPs in GQDs, a novel strategy for developing an efficient and robust electrochemical sensing platform was established. The electrochemical sensor showed high sensitivity and simplicity for detection of L-Trp.

Analytical performance of Fe_3O_4 MNPs-GQDs-

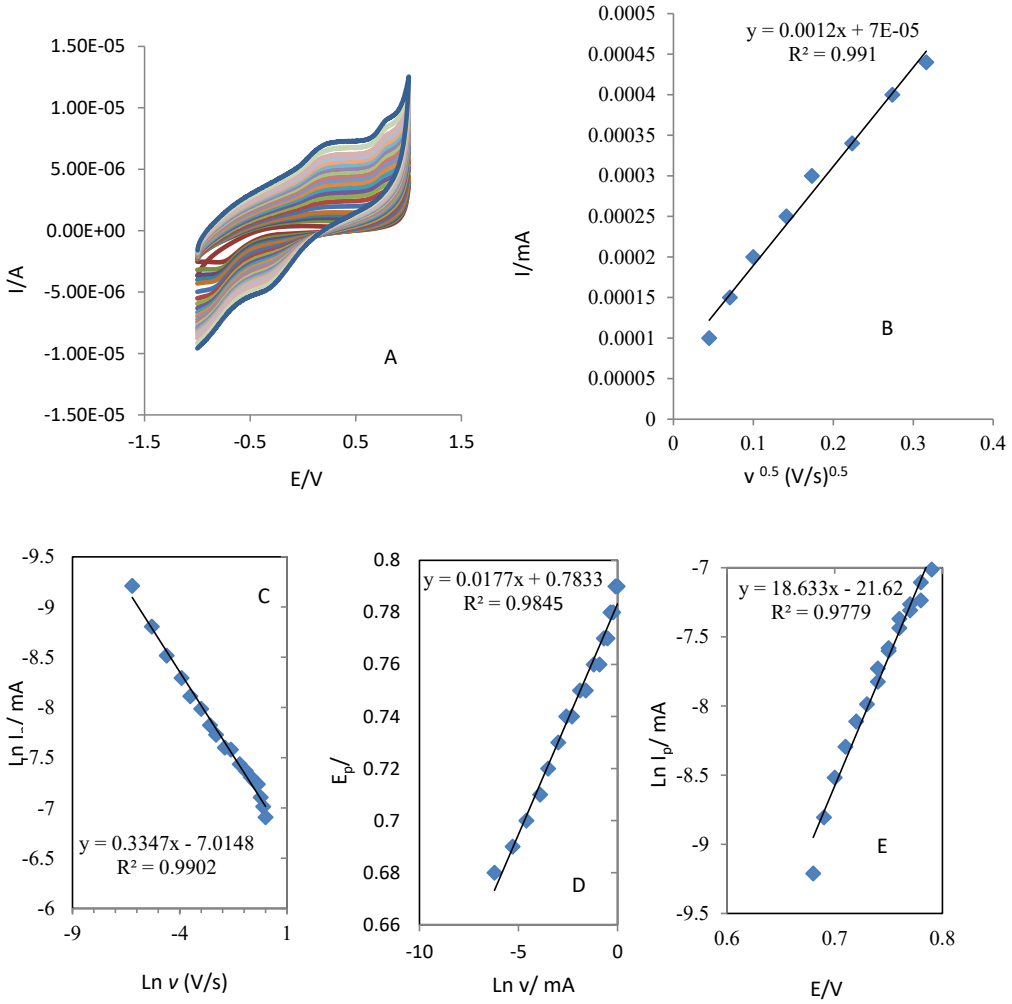

Fig. 6: CVs of Fe_3O_4 MNP-GQDs-GCE in different scan rate (2, 4, 6, 8, 10, 15, 20, 25, 30, 35, 40, 45, 50, 60, 70, 80, 90, 100, 125, 150, 175, 200, 250, 300, 350, 400, 450, 500, 550, 600, 650, 700, 750, 800, 850, 900, 950 and 1000 mV/s) in the presence of 0.1M PBS; B) Variations of oxidation peak currents versus square root of scan rate; C) Variations of oxidation neperian logarithm of peak currents versus neperian logarithm of scan rate; D) Variations of oxidation peak currents versus scan rate (at low scan rates). E) The plot of oxidation and reduction neperian logarithm peak currents (mA) versus peak potential (V). F) The plot of oxidation peak potentials (V) versus neperian logarithm of scan rate.

GCE has been compared with other reported electrodes and the results are shown in Table 1 [14-25]. Binuclear manganese (II) complex modified CPE requires 60.0 s accumulation times prior to the determination of Trp and moreover, the energy required to oxidize Trp at this electrode was more as compared to Fe_3O_4 MNPs-GQDs-GCE [15]. The preparation of carbon nanofibers (CNFs) needs sophistication and apart from that none of the analytical applications of CNF-CPE have been reported [16]. Acidic medium was required for the electrocatalysis of CILE towards Trp [17]. An accumulation time of 1100.0 s and 180.0 s was required for the determination of Trp at CPE/SiO_2 [18] and ERGO/GCE [19] respectively. PAA/GCE suffers serious interference from tyrosine (Tyr) [20]. This setback was not observed at MCPE/MWCNTs. Trp oxidation at CoSal-CNTPE required a very high oxidation over potential [21]. Ag@C core-shell nanocomposites preparation was tedious and it required an electrochemical pre-treatment of glassy carbon electrode prior to the preparation of Ag@C/GCE [22]. The oxidation overpotential at expensive BDD NWs [23]. was very high and it required a highly basic medium for the electrocatalytic oxidation of Trp. A two-step procedure was involved in the preparation of GNP/CILE [24]. The Fe_3O_4 MNPs-GQDs-GCE has certain

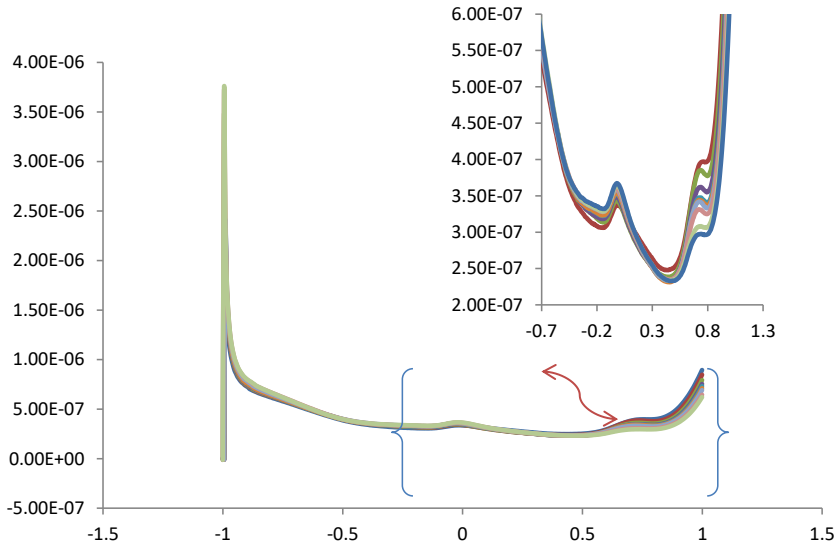

Fig. 7. DPVs of Fe_3O_4 MNP-GQDs-GCE in the presence of L-Trp at different concentrations (0.1, 0.2, 0.3, 0.4, 0.5, 0. 7, 0. 8, 0. 9 and 1µM (From inner to outer).

advantages as compared to glassy carbon (GC) electrode modified with MWCNTs; GC/MWCNT. [24] The GC/MWCNT requires an accumulation time before each measurement while Fe_3O_4 MNPs-GQDs-GCE has an advantage of easily preparation and accumulation time is not required before any measurement. The electrochemical oxidation of Trp was observed at 0.97 V by GC/MWCNT while the same by Fe_3O_4 MNPs-GQDs-GCE were observed at 0.657 V. Hence, L-Trp requires less oxidation over potential at Fe_3O_4 MNPs-GQDs-GCE as compared to GC/MWCNT. The detection limit of Trp at GC/MWCNT was 27 nM. The detection limit achieved at Fe_3O_4 MNPs-GQDs-GCE was comparable with that achieved at GC/MWCNT apart from having an additional advantage of achieving it at physiological pH. Comparing with most of the aforementioned modified electrodes, a much better current sensitivity and wide linear dynamic range is achieved at Fe_3O_4 MNPs-GQDs-GCE without involving any complicated and time-consuming methods of preparation. The oxidation over potential of L-Trp was considerably reduced at Fe_3O_4 MNPs-GQDs-GCE under physiological conditions and so we can easily extend its applications to biological fields. These facts make Fe_3O_4 MNPs-GQDs-GCE a potential electrochemical sensor for the determination of L-Trp for various applications.

Table 1. Comparison of Fe_3O_4 MNPs-GQDs-GCE with other working electrodes.

Electrode.	pH	Linear range (µM)	Detection limit (µM)	Technique used	Refs
CPE/binuclear manganese(II) complex	4.1	0.1-1	0.08	LSV	15
CNF-CPE	7.0	0.1-119	0.1	Amperometry	16
CILE	2.8	8-1000	0.48	CV	17
CPE/SiO_2	2.0	0.1-5	0.36	LSV	18
ERGO/GCE	6.5	0.2-40	0.1		19
PAA/GCE	7.4	1-500	0.081	DPV	20
CoSal-CNTPE	4.0	0.5-50	0.1		21
Ag@C/GCE	2.0	0.1-100	0.04	LSV	22
BDD NWs	11.0	0.5-50	0.5	DPV	23
GNP/CILE	7.0	5-900	4	SWV	24
Fe_3O_4 MNP-GQDs-GCE	7.4	0.08-150	0.08	DPV	This work

CONCLUSION

In conclusion, we have expanded application of Fe_3O_4 MNPs-GQDs-GCE [toward detection and determination of L-Try. In this work, we have described a simple and rapid voltammetric method for the quantification of L-Trp under physiological pH by modifying the GCE with Fe_3O_4 MNPs-GQDs. Decrease in oxidation overpotential and enhancement in current proved the electrocatalytic activity of Fe_3O_4 MNPs-GQDs-GCE as a sensor. Importantly, by this simple method of fabrication a much lower detection limit was achieved without involving any pre-treatment or activation steps. The analytical applicability of the modified electrode has been evaluated by successfully employing it for the determination of L-Trp in the standard solution.

ACKNOWLEDGMENTS

We gratefully acknowledge the partial financial support by Tabriz University of Medical Sciences.

CONFLICT OF INTEREST

The authors declare that there are no conflicts of interest regarding the publication of this manuscript.

REFERENCES

1. Fiorucci AR, Cavalheiro ETG, The use of carbon paste electrode in the direct voltammetric determination of tryptophan in pharmaceutical formulations. J. Pharm. Biomed. Anal. 2002; 28: 909-915
2. Moffat AC, Jackson JV, Moss MS, Widdop B: Clarke's Isolation and Identification of Drugs, The Pharmaceutical Press, London, UK 1986; 1056.
3. Kochen W, Steinhart H, L-Try-Current Prospects in Medicine and Drug Safety; de-Gruyter: Berlin, 1994.
4. Akhgar MR, Salari M, Zamani H, Simultaneous determination of levodopa, NADH, and tryptophan using carbon paste electrode modified with carbon nanotubes and ferrocenedicarboxylic acid J. Solid State Electrochem. 2011; 15: 845-853
5. Deo RP, Lawrence NS, Wang J, Electrochemical detection of amino acids at carbon nanotube and nickel-carbon nanotube modified electrodes. Analyst 2004; 129: 1076-1081
6. Dong S, Zhang S, Chi L, He P, Wang Q, Fang Y, Electrochemical behaviors of amino acids at multiwall carbon nanotubes and Cu2O modified carbon paste electrode. Anal. Biochem. 2008; 381: 199-204
7. Liu X, Luo L, Ding Y, Kang Z, Ye D, Simultaneous determination of L-cysteine and L-tyrosine using Au-nanoparticles/poly-eriochrome black T film modified glassy carbon electrode. Bioelectrochemistry 2012; 86: 38-45
8. MacDonald SM, Roscoe SG, Electrochemical oxidation reactions of tyrosine, tryptophan and related dipeptides. Electrochim. Acta 1997; 42: 1189-1200
9. Ye D, Luo L, Ding Y, Liu B, Liu X, Fabrication of Co_3O_4 nanoparticles-decorated graphene composite for determination of L-tryptophan. Analyst 2012; 137: 2840-2845
10. Nan CG, Feng ZZ, Li WX, Ping DJ, Qin CH, Electrochemical behavior of tryptophan and its derivatives at a glassy carbon electrode modified with hemin. Anal. Chim. Acta 2002; 452: 245-254
11. Guo Y, Guo S, Fang Y, Dong S, Gold nanoparticle/carbon nanotube hybrids as an enhanced material for sensitive amperometric determination of tryptophan. Electrochim. Acta 2010; 55: 3927-3931
12. Hasanzadeh M, karimzadeh A, Shadjou N, Mokhtarzadeh A, Bageri L, Sadeghi S, Mahboob S, Graphene quantum dots decorated with magnetic nanoparticles: Synthesis, electrodeposition, characterization and application as an electrochemical sensor towards determination of some amino acids at physiological pH. Mater. Sci. Engin. C 2016; 68: 814-830
13. Bard AJ, Faulkner LR, Electrochemical methods: fundamentals and applications, 2nd ed., John Wiley & Sons, New York, 2001; pp. 236, 503, 709
14. Hasanzadeh M, Sadeghi S, Bageri L, Mokhtarzadeh A, Karimzadeh A, Shadjou N, Mahboob S. Poly-dopamine-beta-cyclodextrin: a novel nanobiopolymer towards sensing of some amino acids at physiological pH, Mater Sci. Eng. C 2016; 69: 343-357.
15. Xu J, Yuan Y, Li W, Deng P, Deng J, Carbon paste electrode modified with a binuclear manganese complex as a sensitive voltammetric sensor for tryptophan. Microchim. Acta 2011; 174: 239-245
16. Tang X, Liu Y, Hou H, You T, Electrochemical determination of L-Tryptophan, L-Tyrosine and L-Cysteine using electrospun carbon nanofibers modified electrode. Talanta 2010; 80: 2182-2186
17. Jiang Q, Sun W, Jiao K, Electrochemical behavior and determination of L-tryptophan on carbon ionic liquid electrode. J. Anal. Chem. 2010; 65: 648-651
18. Xu M, Ma M, Ma Y, Electrochemical determination of tryptophan based on silicon dioxide nanopartilces modified carbon paste electrode. Russ. J. Electrochem. 2012; 48: 489-494
19. Güney S, Yıldız G, Determination of tryptophan using electrode modified with poly(9-aminoacridine) functionalized multi-walled carbon nanotubes. Electrochim. Acta 2011; 57: 290-296
20. Shahrokhian S, Fotouhi L, Carbon paste electrode incorporating multi-walled carbon nanotube/cobalt salophen for sensitive voltammetric determination of tryptophan. Sens. Actuat. B 2007; 123: 942-949
21. Mao S, Li W, Long Y, Tu Y, Deng A, Sensitive electrochemical sensor of tryptophan based on Ag@C core-shell nanocomposite modified glassy carbon electrode. Anal. Chim. Acta, 2012; 738: 35-40
22. Deng K.Q, Zhou J.-H, Li X.-F, Direct electrochemical reduction of graphene oxide and its application to determination of L-tryptophan and L-tyrosine. Colloids Surf. B., 2013; 101: 183-188
23. Szunerits S, Coffinier Y, Galopin E, Brenner J, Boukherrou R, Preparation of boron-doped diamond nanowires and their application for sensitive electrochemical detection of tryptophan. Electrochem. Commun. 2010; 12; 438-441
24. Safavi A, Momeni S. Electr0ocatalytic Oxidation of Tryptophan at Gold Nanoparticle-Modified Carbon Ionic Liquid Electrode. Electroanalysis, 2010; 22: 2848-2855.